

parasite development at the late schizont stage, as measured by an increase in schizonts. High concentrations of E-64d also induced a massive enlargement of the food vacuole within parasites, which is consistent with previously reported effects of general cysteine protease inhibitors (24) (Fig. 4B, middle panel). In contrast, falcipain 1-specific inhibitors caused a similar dose-dependent decrease in the percentage of new ring-stage parasites (Fig. 4A, blue bars), but did not block schizont development and subsequent rupture as indicated by the appearance of merozoites (Fig. 4B, right panel). Furthermore, schizont rupture was not affected, as assessed by the constant number of schizonts at all concentrations of falcipain 1-specific inhibitor (Fig. 4A) and by measurement of the release of the parasitophorous vacuolar protein SERA (serine repeat antigen) (25). These results suggest that falcipain 1 is not involved in hemoglobin degradation or red blood cell rupture at the end of schizogony, but rather has a specific role in the invasion of red blood cells by extracellular merozoites.

We have shown, using a functional proteomics screen combined with a chemical genetic approach, that falcipain 1 functions dur-

ing the process of host cell invasion during the erythrocytic cycle of *P. falciparum*. The primary sequence of falcipain 1 is well conserved across the *Plasmodium* genus (26), making it a potentially useful new target for design of therapeutic drugs in all four plasmodial species that cause malaria in humans. Therapeutic agents that are able to specifically prevent or slow the process by which merozoites infect new cells are likely to disrupt the development cycle and allow time for the host immune response to destroy the extracellular parasite.

References and Notes

1. P. J. Rosenthal, G. K. Lee, R. E. Smith, *J. Clin. Invest.* **91**, 1052 (1993).
2. J. H. McKerrow, J. C. Engel, C. R. Caffrey, *Bioorg. Med. Chem.* **7**, 639 (1999).
3. J. C. Engel, P. S. Doyle, I. Hsieh, J. H. McKerrow, *J. Exp. Med.* **188**, 725 (1998).
4. B. R. Shenai, P. S. Sijwali, A. Singh, P. J. Rosenthal, *J. Biol. Chem.* **275**, 29000 (2000).
5. P. S. Sijwali, B. R. Shenai, J. Gut, A. Singh, P. J. Rosenthal, *Biochem. J.* **360**, 481 (2001).
6. P. Raphael et al., *Mol. Biochem. Parasitol.* **110**, 259 (2000).
7. B. L. Salmon, A. Oksman, D. E. Goldberg, *Proc. Natl. Acad. Sci. U.S.A.* **98**, 271 (2001).
8. R. Mayer et al., *J. Med. Chem.* **34**, 3029 (1991).
9. X. Que et al., *J. Biol. Chem.* **277**, 25791 (2002).
10. L. H. Bannister, G. H. Mitchell, G. A. Butcher, E. D. Dennis, S. Cohen, *Cell Tissue Res.* **245**, 281 (1986).
11. D. Greenbaum, K. F. Medzihradzky, A. Burlingame, M. Bogyo, *Chem. Biol.* **7**, 569 (2000).

12. D. Greenbaum et al., *Mol. Cell Proteomics* **1**, 60 (2002).
13. D. Greenbaum et al., *Chem. Biol.*, **9**, 1085 (2002).
14. M. Hanspal, V. K. Goel, S. S. Oh, A. H. Chishty, *Mol. Biochem. Parasitol.* **122**, 227 (2002).
15. M. J. Gardner et al., *Science* **282**, 1126 (1998).
16. S. Bowman et al., *Nature* **400**, 532 (1999).
17. A. Bahl et al., *Nucleic Acids Res.* **30**, 87 (2002).
18. P. J. Rosenthal, R. G. Nelson, *Mol. Biochem. Parasitol.* **51**, 143 (1992).
19. F. Salas, J. Fichmann, G. K. Lee, M. D. Scott, P. J. Rosenthal, *Infect. Immun.* **63**, 2120 (1995).
20. C. E. Chitnis, M. J. Blackman, *Parasitol. Today* **16**, 411 (2000).
21. D. C. Greenbaum, M. Bogyo, unpublished data.
22. D. C. Greenbaum, J. Engel, A. A. Holder, M. Bogyo, unpublished data.
23. Cluster, version 2.11; TreeView, version 1.50, M. B. Eisen, P. T. Spellman, P. O. Brown, D. Botstein, *Proc. Natl. Acad. Sci. USA.* **95**, 14863 (1998) (available at <http://rana.lbl.gov>).
24. P. J. Rosenthal, J. H. McKerrow, M. Aikawa, H. Nagasawa, J. H. Leech, *J. Clin. Invest.* **82**, 1560 (1988).
25. D. Greenbaum, A. Holder, M. Bogyo, unpublished data.
26. P. J. Rosenthal, P. S. Sijwali, A. Singh, B. R. Shenai, *Curr. Pharm. Des.* **8**, 1659 (2002).
27. We thank J. McKerrow, P. Rosenthal, and C. C. Wang (University of California, San Francisco) for critical evaluation of the manuscript. Supported by funding from the Sandler Program in Basic Sciences (M.B.).

Supporting Online Material

[www.sciencemag.org/cgi/content/full/298/5600/2002/DC1](http://www.sciencemag.org/cgi/content/full/298/5600/2002/DC1)

Materials and Methods  
References and Notes

16 August 2002; accepted 15 October 2002

## Signaling of Rat Frizzled-2 Through Phosphodiesterase and Cyclic GMP

Adriana Ahumada,<sup>1</sup> Diane C. Slusarski,<sup>2</sup> Xunxian Liu,<sup>1</sup> Randall T. Moon,<sup>3</sup> Craig C. Malbon,<sup>1</sup> Hsien-yu Wang<sup>4\*</sup>

The Frizzled-2 receptor (Rfz2) from rat binds Wnt proteins and can signal by activating calcium release from intracellular stores. We show that wild-type Rfz2 and a chimeric receptor consisting of the extracellular and transmembrane portions of the  $\beta_2$ -adrenergic receptor with cytoplasmic domains of Rfz2 also signaled through modulation of cyclic guanosine 3',5'-monophosphate (cGMP). Activation of either receptor led to a decline in the intracellular concentration of cGMP, a process that was inhibited in cells treated with pertussis toxin, reduced by suppression of the expression of the heterotrimeric GTP-binding protein (G protein) transducin, and suppressed through inhibition of cGMP-specific phosphodiesterase (PDE) activity. Moreover, PDE inhibitors blocked Rfz2-induced calcium transients in zebrafish embryos. Thus, Frizzled-2 appears to couple to PDEs and calcium transients through G proteins.

The Wnt proteins are secreted signaling proteins that play diverse roles in cell polarity, cell proliferation, and specification of cell fate (1–3). Wnt proteins signal through *frizzled* (Fz) gene products (4, 5), members of the superfamily of G-protein-coupled receptors (GPCRs) (6–8). Wnt-Fz family members can be grouped into functionally distinct classes. Activation of the Wnt- $\beta$ -catenin pathway increases nuclear accumulation of the Lef-Tcf transcriptional coactivator  $\beta$ -catenin (1, 2, 9), thus activating transcrip-

tion (10–14). The Rfz2 receptor, by itself, transduces binding of Wnt-5A to increases in intracellular calcium release (15) and activation of calcium-calmodulin-dependent protein kinase II (16, 17) and protein kinase C (18) without appreciably activating the canonical Wnt- $\beta$ -catenin pathway. Because purified, active Wnt proteins are not available for analysis of Rfz2 receptor function, we engineered a chimeric receptor to substitute the three cytoplasmic loops and the COOH-terminal tail of the Rfz2 receptor for the

corresponding regions of the hamster  $\beta_2$ -adrenergic receptor ( $\beta_2$ AR) (19). The Rfz2 chimeric receptor, whose cytoplasmic domains display no similarity to that of  $\beta_2$ AR (fig. S1A) (20), is functional insofar as it couples to calcium mobilization (19) and to rapid activation of calcium-calmodulin-dependent kinase II (16), as does the wild-type Rfz2.

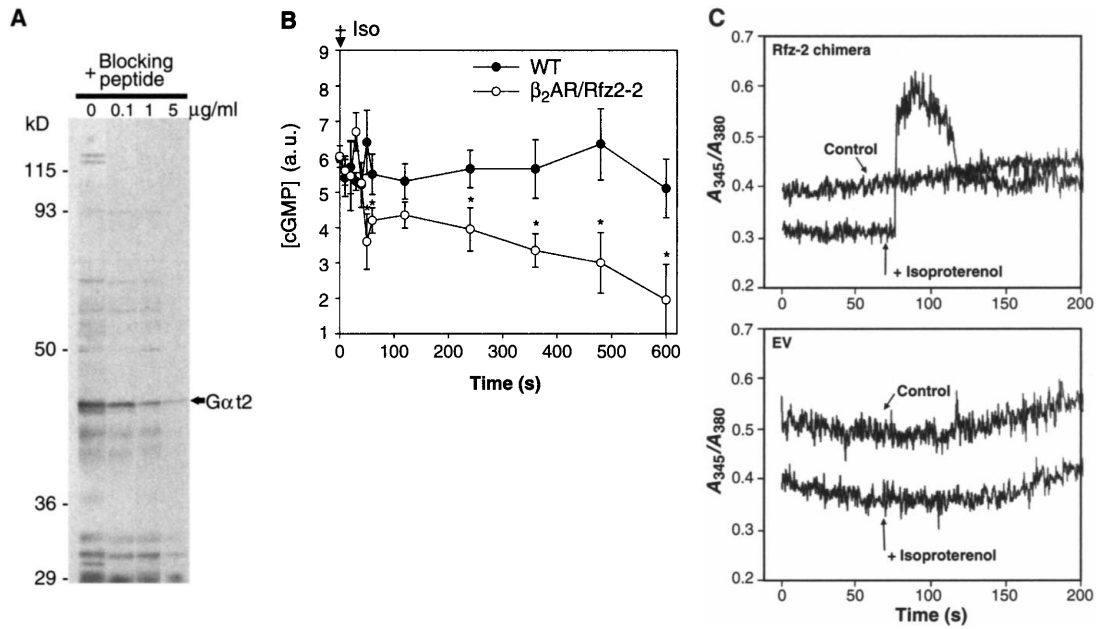
For functional analysis of Rfz2 signaling, we expressed the Rfz2 chimera in mouse totipotent F9 teratocarcinoma cells and in Chinese hamster ovary (CHO) cells that lack endogenous  $\beta_2$ AR. We identified stable transfectants expressing the Rfz2 chimera in CHO clones by reverse transcription (RT) and polymerase chain reaction (PCR) amplification (fig. S1B) (19, 20), immunoblotting with antibodies to  $\beta_2$ AR (fig. S1C) (19, 20), and specific binding of the  $\beta_2$ AR antagonist [<sup>125</sup>I]iodo-

<sup>1</sup>Department of Molecular Pharmacology, Diabetes and Metabolic Diseases Research Center, University Medical Center, SUNY–Stony Brook, Stony Brook, NY 11794–8651, USA. <sup>2</sup>Department of Biological Sciences, University of Iowa, Iowa City, IA 52242, USA. <sup>3</sup>Howard Hughes Medical Institute, Department of Pharmacology and Center for Developmental Biology, University of Washington School of Medicine, Seattle, WA 98195, USA. <sup>4</sup>Department of Physiology and Biophysics, Diabetes and Metabolic Diseases Research Center, University Medical Center, SUNY–Stony Brook, Stony Brook, NY 11794–8661, USA.

\*To whom correspondence should be addressed. E-mail: [wangh@pharm.sunysb.edu](mailto:wangh@pharm.sunysb.edu)

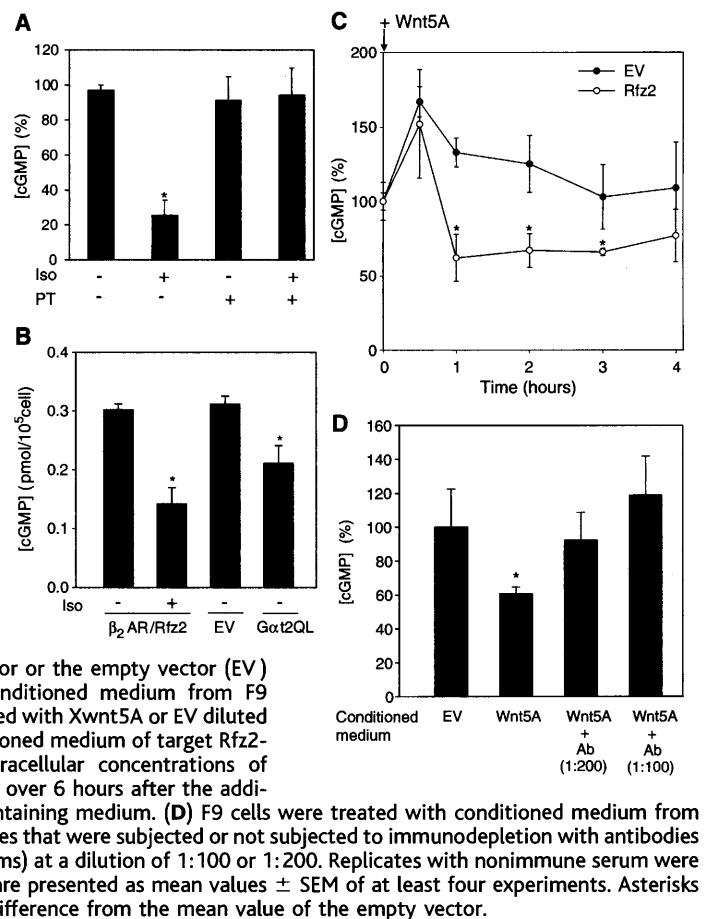
REPORTS

**Fig. 1.** Expression of *Gat2* links the Rfz2 chimera to changes in intracellular concentrations of cGMP. **(A)** Proteins from crude membranes prepared from F9 cells were subjected to SDS-polyacrylamide gel electrophoresis and transferred to nitrocellulose. The blots stained with antibodies specific for *Gat2*. Antibodies to *Gat2* were incubated in advance without or with immunizing peptide (0.1, 1.0, and 5.0  $\mu\text{g/ml}$ ) used to create the antibody. **(B)** Intracellular concentrations of cGMP were determined in wild-type F9 cells and clones expressing the Rfz2 chimera receptors treated with 10  $\mu\text{M}$  isoproterenol. Clone  $\beta_2\text{AR/Rfz2}$  was analyzed for intracellular concentrations of cGMP. Data shown are mean values  $\pm$  SEM from three experiments. Asterisks denote differences from the level at time 0 with a  $P$  value of  $<0.05$  (SigmaStat software, SPSS Science). **(C)** Measurements of intracellular  $\text{Ca}^{2+}$  with Fura-2. Clones expressing either the Rfz2 chimera receptor or harboring the empty vector (EV) were



cyanopindolol (ICYP) (fig. S1D) (20). The pharmacological properties of the Rfz2 chimera measured by binding of the labeled antagonist ICYP were very similar to those of native  $\beta_2\text{AR}$  (fig. S1E and table S1) (20); however, the chimeric receptor did not stimulate cyclic adenosine 3',5'-monophosphate accumulation (19), as does the native  $\beta_2\text{AR}$  (7). Depletion of the G protein  $\alpha$  subunit *Gat2* abolished signaling of the Rfz2 receptor in mouse F9 cells (19). This putative role of *Gat2* was surprising, because *Gat1* and *Gat2* are expressed predominantly in visual tissues (21). Therefore, we explored *Gat2* expression in mouse F9 and in CHO cells. As analyzed by RT-PCR amplification, we observed *Gat2* expression in both of these embryonic cell lines (fig. S2A) (20). Direct sequencing of the PCR products confirmed the identity of *Gat2* (22). We also analyzed *Gat2* protein expression in crude membrane fractions prepared from mouse F9 cells with immunoblotting by using *Gat2*-specific polyclonal antibody to peptide (Fig. 1A). Immunoreactivity was observed with a relative mobility of *Gat2* ( $\sim 40$  kD). The competing peptide used as the immunogen effectively blocked recognition of the putative *Gat2* by the antibody to *Gat2* in a dose-dependent manner (Fig. 1A). Immunoblots of F9 cells as well as CHO cells that were transiently transfected with a mammalian expression vector harboring the Q204L (Gln<sup>204</sup> to Leu) mutant form of *Gat2* demonstrated the appearance of additional  $\sim 40$ -kD immunoreactive material (22). Thus, at the RNA and protein levels,

**Fig. 2.** Effects of pertussis toxin and constitutively activated *Gat2* on intracellular concentrations of cGMP. **(A)** F9 clones expressing the Rfz2 chimera were treated with pertussis toxin (Pt) (10 ng/ml) overnight and then treated with isoproterenol (10  $\mu\text{M}$  Iso). **(B)** F9 clones were transiently transfected with an expression vector harboring the constitutively activated mutant form Q204L of *Gat2* (*Gat2*QL). Asterisks denote differences from the wild-type cells in the absence of isoproterenol with a  $P$  value of  $<0.05$ . **(C)** F9 clones expressing Rfz2 receptor or the empty vector (EV) were treated with conditioned medium from F9 clones stably transfected with Xwnt5A or EV diluted in nine parts of conditioned medium of target Rfz2-expressing clones. Intracellular concentrations of cGMP were monitored over 6 hours after the addition of the Wnt5A-containing medium. **(D)** F9 cells were treated with conditioned medium from Xwnt5A-secreting clones that were subjected or not subjected to immunodepletion with antibodies to Wnt5A (R+D Systems) at a dilution of 1:100 or 1:200. Replicates with nonimmune serum were not prepared. Results are presented as mean values  $\pm$  SEM of at least four experiments. Asterisks denote  $P < 0.05$  for difference from the mean value of the empty vector.



*Gat2* appears to be expressed in both F9 and CHO cells. Because the only known effector for *Gat* is a phosphodiesterase (PDE), we ex-

amined the effects of activation of the Rfz2 chimera on the intracellular concentration of cGMP in F9 cells. Stimulation of the Rfz2 chimera with the  $\beta_2\text{AR}$  agonist iso-

## REPORTS

proteranol resulted in decreased concentration of intracellular cGMP within the first minute after administration (Fig. 1B). We investigated three independent Rfz2 chimera-bearing F9 clones and each displayed a similar response (fig. S2B) (20). cGMP concentrations in wild-type F9 cells, in contrast, were unaffected by treatment with isoproterenol. Stimulation of Rfz2 leads to an increase in intracellular calcium concentrations in zebrafish embryos (15, 19, 23), as did activation of the Rfz2 chimera in F9 cells (Fig. 1C). The cGMP response in F9 cells was dose responsive with respect to isoproterenol, achieving maximal stimulation at 1  $\mu$ M (fig. S2C), similar to dose-responses curves for other Rfz2 chimera-mediated responses (19, 20).

G $\alpha$ t2, a member of the G $\alpha$ i-protein family, is a substrate for pertussis toxin-catalyzed inactivation (7). Therefore, we investigated the effects of toxin treatment on the Rfz2 chimera-mediated cGMP response. Treating F9 cells with pertussis toxin overnight attenuated by >85% the decline in cGMP concentration noted in response to activation of the chimeric Rfz2 (Fig. 2A). Also, expression of the constitutively active Q204L mutant of G $\alpha$ t2, which lacks intrinsic guanosine triphosphatase activity, provoked a decline in the steady-state concentration of intracellular cGMP (Fig. 2B), demonstrating another direct linkage between G $\alpha$ t2 and cGMP levels in these mammalian embryonic carcinoma cells.

F9 cells expressing the wild-type Rfz2 receptor responded to conditioned medium from Wnt-5A-secreting F9 cells with a change in intracellular cGMP levels (Fig. 2C). The time course of the cGMP response to Wnt-5A-containing conditioned medium was slower than the response observed for activation of the Rfz2 chimera. We observed an initial increase in cGMP levels within 30 min of challenge in Rfz2-expressing cells (as well as F9 cells lacking Rfz2 receptors), which suggests that other components in the conditioned medium could activate guanylyl cyclase. Over time, the cGMP response to Wnt-5A attenuated, a phenomenon that might reflect degradation of the Wnt ligand. Treating the conditioned medium from the Wnt-5A-expressing cells with antibodies to Wnt-5A resulted in immunodepletion of Wnt-5A from the medium and loss of the cGMP response (Fig. 2D). Treatment with conditioned medium from Wnt-8-expressing F9 cells failed to stimulate a decrease in the concentration of cGMP (22).

Guanosine triphosphate (GTP) stimulates the activation and dissociation of GPCR from their cognate G proteins, which results in a decrease in the affinity of the receptor for agonist (Fig. 3A). Agonist competition curves for Rfz2 chimera dis-

played an agonist-specific shift in receptor affinity in the presence of the hydrolysis-resistant analog of GTP, guanosine 5'-O-(3'-thiotriphosphate) (GTP- $\gamma$ -S) (50  $\mu$ M, Fig. 3B). These data are consistent with a molecular interaction between Rfz2 chimera and G proteins. Overnight treatment of cells with pertussis toxin attenuated the GTP-induced shift, implicating pertussis toxin-sensitive members of the G $\alpha$ i family (for example, G $\alpha$ i1, -2, -3; G $\alpha$ o; and G $\alpha$ t). Depletion of G $\alpha$ t with antisense ODNs produced a rightward shift in the agonist competition curve in the absence or presence of GTP- $\gamma$ -S (Fig. 3C), whereas depletion of an unrelated G protein, G $\alpha$ s, did not alter the agonist-specific shift of Rfz2 chimera affinity in response to GTP- $\gamma$ -S (Fig. 3D), although the antisense oligodeoxynucleotides (ODNs) suppressed the expression of these G protein  $\alpha$  subunits by 60% to 90% (fig. S3) (20).

We used RT-PCR to demonstrate that

F9 cells express cGMP-selective PDEs, PDE6 and PDE10 (Fig. 4A). We established expression of PDE5 $\alpha$  and PDE6 $\alpha$  by immunoblotting with antibodies to bovine PDEs isolated and purified from the eye (Fig. 4B).

Mouse F9 cells are used as a model to study early mouse development and can be induced by retinoic acid and other agents to form primitive endoderm (PE), a phenotype characterized by expression of markers such as cytokeratin endo A and tissue plasminogen activator (24). We examined the ability of pharmacological inhibitors of PDE to prevent changes in cGMP concentrations in F9 cells (Fig. 4C) and to block the Rfz2 chimera-induced formation of primitive endoderm in these F9 clones (Fig. 4D). Treatment of F9 cells expressing the Rfz2 chimera with a PDE inhibitor [0.5 mM methylisobutyl xanthine (MIX), 1  $\mu$ M dipyridamole, or 1  $\mu$ M zaprinast] caused increases in the intracellular concentration

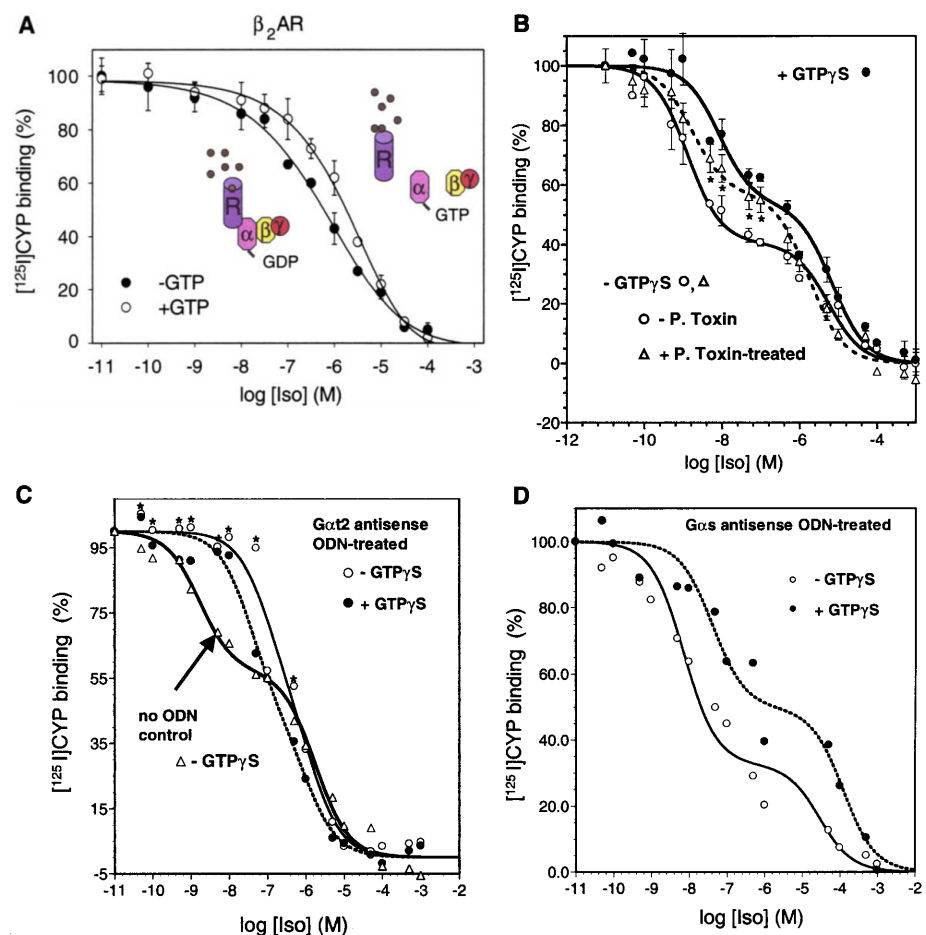


**Fig. 3.** Sensitivity of agonist binding of Rfz2 chimera to pertussis toxin and to suppression of G $\alpha$ t2. (A) Crude membranes were prepared from CHO clones expressing the Rfz2 chimera and assayed for the ability of isoproterenol to compete in radioligand binding assays with the labeled antagonist ICYP in the presence and absence of GTP- $\gamma$ -S. Clones expressing the Rfz2 chimera were treated overnight with pertussis toxin (10 ng/ml) (B) or with antisense ODNs targeting either G $\alpha$ t2 (C) or G $\alpha$ s (D). Asterisks denote differences of ICYP binding between treated and untreated control with *P* values of <0.05.

## REPORTS

of cGMP (Fig. 4C). Furthermore, the Rfz2-mediated decline in cGMP was abolished in the presence of the PDE inhibitors. When cells were treated at higher concentrations of PDE inhibitors (10  $\mu$ M dipyrindamole or zaprinast), cGMP levels increased two- to threefold over basal levels (22). Staining with the TROMA-1 monoclonal antibody that recognizes cytokeratin endo A, a hallmark of PE, showed that the inhibitors blocked PE formation in response to activation of the Rfz2 chimera with isoproterenol (Fig. 4D, table S2) (20).

Ectopic expression of Rfz2 RNA in zebrafish induces an increase in intracellular calcium release in vivo and the modulation of calcium release is pertussis toxin sensitive (15). Therefore, we investigated whether PDE activity is required for Rfz2-induced increases in calcium release in the developing zebrafish embryo. Zebrafish embryos at the one-cell stage were injected with Rfz2 RNA mixed with Fura-2-dextran, a calcium-sensing dye that is excluded from

intracellular organelles. We subjected the embryos to fluorescence ratio imaging during early development to determine the spatial and temporal dynamics of calcium release (Fig. 5A). Embryos were monitored to determine Rfz2-induced calcium release activity (Fig. 5B). Some embryos were injected at the 8- to 16-cell stage with 50  $\mu$ M dipyrindamole (Fig. 5C) or 10  $\mu$ M zaprinast (Fig. 5D) in combination with lineage marker Texas Red-dextran. Rfz2 RNA injection increases the frequency of calcium release two- to threefold over endogenous activity (Fig. 5A) (15). The Rfz2-induced calcium fluxes are inhibited by exposure to dipyrindamole (Fig. 5C) ( $n = 7$ ) or zaprinast (Fig. 5D) ( $n = 4$ ). The range of inhibition extended beyond the Texas Red-positive region, suggesting diffusion of the drug. Reducing the dipyrindamole dose to 15  $\mu$ M led to local, partial inhibition of Rfz2-induced calcium fluxes (22).

Movements during zebrafish gastrulation position cells at the future dorsal side

and subsequently extend and narrow the embryo along the anterior-posterior (A-P) axis. Genetic mutations for components of the Wnt-Ca<sup>2+</sup> pathway have been identi-

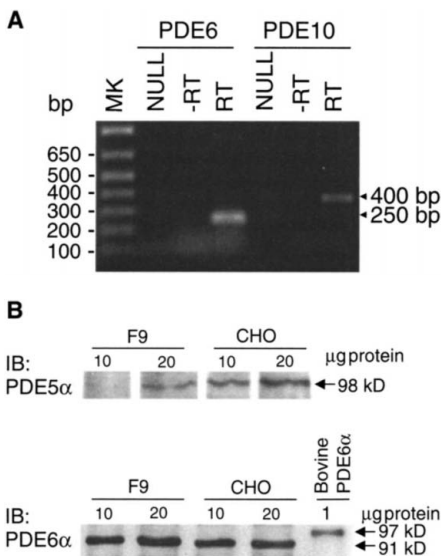


**Fig. 4.** Expression of PDE5, PDE6, and PDE10 in CHO and F9 stem cells. F9 or CHO cells were examined for the expression of various PDE $\alpha$  subunits by RT-PCR and immunoblotting. (A) For RT-PCR, the reaction mixtures included those without template (Null), a sample of RNA without prior RT (-RT), and RT products of whole-cell RNA samples (RT) from F9 cells. (B) Proteins of samples of whole-cell extracts from F9 or CHO were subjected to SDS-polyacrylamide gel electrophoresis and blotting followed by staining with antibodies specific to either PDE5 $\alpha$  or PDE6 $\alpha$ . (C) Effects of PDE5 and PDE6 selective inhibitors dipyrindamole (Dipy, 1  $\mu$ M), zaprinast (Zap, 1  $\mu$ M), and MIX (0.5 mM) on intracellular concentrations of cGMP in F9 cells after a 30-min incubation. (D) Effects of PDE inhibitors MIX (0.5 mM), Dipy (10  $\mu$ M), Zap (10  $\mu$ M), or the MEK inhibitor PD98059 (PD, 5  $\mu$ M) on Rfz2 chimera-induced formation of primitive endoderm. Clones were treated with isoproterenol (+Iso, 10  $\mu$ M) and examined after 3 days for expression of cytokeratin endo A with the TROMA-1 antibody. Results shown are representative of at least three experiments (20).

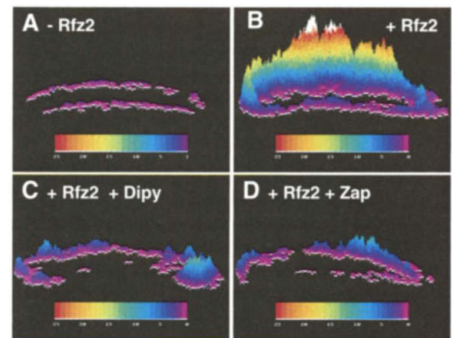
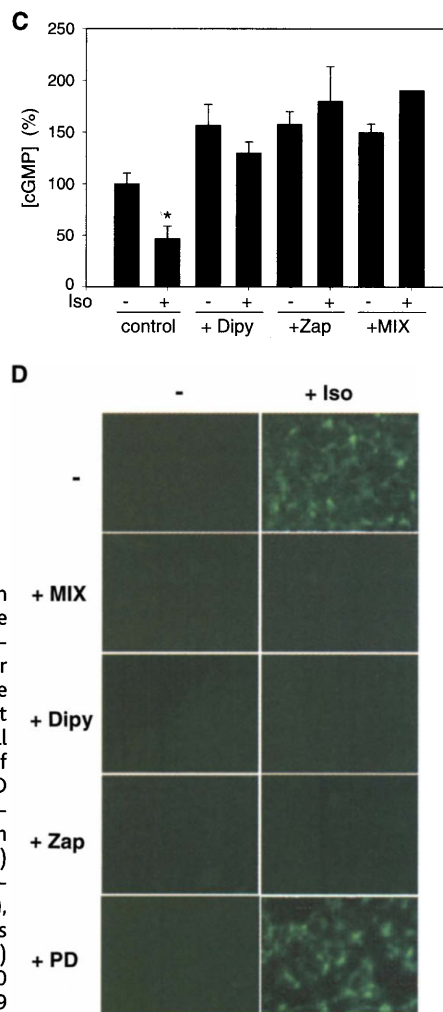


**Fig. 5.** PDE inhibitors block Wnt-Rfz2 signaling in zebrafish embryos. Rfz2 mediates Ca<sup>2+</sup> transients of zebrafish embryos, and these changes in intracellular calcium were monitored with Fura-2. Ratio image data collected from live embryos were processed by a subtractive analog to generate a profile of calcium transients. Calcium release composites from embryos injected without Rfz2 RNA (A), with Rfz2 RNA alone (B), or with Rfz2 RNA in combination with 50  $\mu$ M dipyrindamole (~100 pl) (C) or 10  $\mu$ M zaprinast (~100 pl) (D). A representative embryo is shown for each condition. Panels provide a two-dimensional topographic representation of the location of all the calcium fluxes that occurred during the sampling session (50 min). Peaks and pseudocoloration represent the number of calcium transients that map to the location of the embryo. The embryo is imaged in the lateral orientation. For pseudo-coloring, purple is low (1) and red is high (>25), with peaks representing regions of high activity.

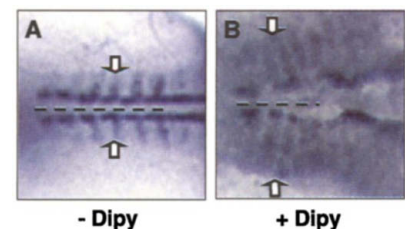
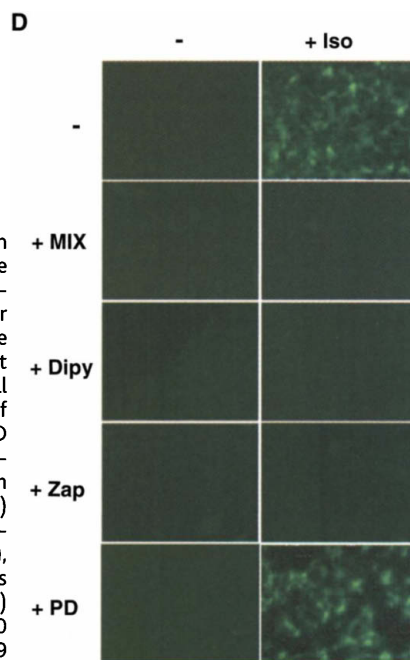


**Fig. 6.** Altered A-P axis length after inhibition of PDE. Zebrafish embryos treated with PDE inhibitor were examined for alteration to A-P axis length by whole mount in situ. Dorsal view of the trunk region of six- to eight-somite stage embryos labeled with the somitic marker *MyoD*. Anterior to the left and arrows demarcate the lateral domain of *MyoD* expression in one pair of somites in wild type (A) and in embryos soaked in 5 to 10  $\mu$ M dipyrindamole (B). Reduced extension of the A-P axis is apparent by the increased density of somites. Dashed lines highlight the length from somite 1 to 6. Somites are packed closer together; thus, the distance is reduced in PDE inhibitor-treated embryos (see fig. S4, B and C). Full details of the whole-mount in situ analysis of *MyoD* expression and alterations in morphology are provided in (20).

fied and have been shown to function in zebrafish gastrulation movements (25, 26). As Wnt activity can stimulate calcium release through activation of Rfz2 (15, 23), we tested whether loss of PDE activity would cause defects in cell movement. Embryos treated with the PDE inhibitors dipyridamole and zaprinast during gastrulation stages lacked extension along the A-P axis, a hallmark for cell movement defects during gastrulation, which results in transient reduction of body length (Fig. 6, table S3) (20). Decreased dorsal convergence was demonstrated by the medial-lateral broadening of *MyoD* expression, a somite marker (27). Relative to wild type (Fig. 6A), we observed severe lateral expansion of *MyoD* expression or epiboly defects in 76% of embryos incubated at doses of 10  $\mu$ M dipyridamole (Fig. 6B) ( $n = 38$ ). We observed moderate defects in embryos (fig. S4A) incubated in lower doses (fig. S4B) (20) ( $n = 90$ ) and less severe defects in zaprinast-treated embryos (fig. S4C) (20) ( $n = 84$ ). Reduced extension of the A-P axis is apparent by the increased density of somites. Dashed lines highlight the length from somite 1 to 6. Somites are packed closer together, and thus the distance is reduced in PDE inhibitor-treated embryos (Fig. 6, A and B; fig. S4, B and C). The full

details of the whole mount in situ analysis of *MyoD* expression and alterations in morphology are provided in (20).

This work identifies a novel role for a signaling pathway that largely was thought to be confined to the visual pathway. Our data reveal a key role of PDE and of cGMP in Wnt-Frizzled signaling (fig. S5) (20). Activation of Rfz2 by Wnt5A leads to activation of G protein-mediated downstream signaling, culminating in the activation of phospholipase C and PDE, integrating calcium and cGMP signaling.

References and Notes

1. K. M. Cadigan, R. Nusse, *Genes Dev.* **11**, 3286 (1997).
2. R. T. Cox, M. Peifer, *Curr. Biol.* **8**, R140 (1998).
3. R. T. Moon, J. D. Brown, M. Torres, *Trends Genet.* **13**, 157 (1997).
4. P. Bhanot et al., *Nature* **382**, 225 (1996).
5. Y. Wang et al., *J. Biol. Chem.* **271**, 4468 (1996).
6. J. Yang-Snyder et al., *Curr. Biol.* **6**, 1302 (1996).
7. A. J. Morris, C. C. Malbon, *Physiol. Rev.* **79**, 1373 (1999).
8. C. C. Malbon, H. Wang, R. T. Moon, *Biochem. Biophys. Res. Commun.* **287**, 589 (2001).
9. D. Cook et al., *EMBO J.* **15**, 4526 (1996).
10. J. Behrens et al., *Science* **280**, 596 (1998).
11. J. Behrens et al., *Nature* **382**, 638 (1996).
12. M. Molenaar et al., *Cell* **86**, 391 (1996).
13. J. Roose et al., *Nature* **395**, 608 (1998).
14. H. Clevers, M. van de Wetering, *Trends Genet.* **13**, 485 (1997).
15. D. C. Slusarski, V. G. Corces, R. T. Moon, *Nature* **390**, 410 (1997).
16. M. Kuhl, L. C. Sheldahl, C. C. Malbon, R. T. Moon, *J. Biol. Chem.* **275**, 12701 (2000).

17. M. Kuhl, L. C. Sheldahl, M. Park, J. R. Miller, R. T. Moon, *Trends Genet.* **16**, 279 (2000).
18. L. C. Sheldahl, M. Park, C. C. Malbon, R. T. Moon, *Curr. Biol.* **9**, 695 (1999).
19. X. Liu et al., *Proc. Natl. Acad. Sci. U.S.A.* **96**, 14383 (1999).
20. Materials and Methods are available as supporting material on Science Online.
21. C. J. Raport, B. Dere, J. B. Hurley, *J. Biol. Chem.* **264**, 7122 (1989).
22. A. Ahumada, D. C. Slusarski, R. T. Moon, C. C. Malbon, H.-y. Wang, unpublished observations.
23. D. C. Slusarski, J. Yang-Snyder, W. B. Busa, R. T. Moon, *Dev. Biol.* **182**, 114 (1997).
24. S. Strickland, *Cell* **24**, 277 (1981).
25. C. P. Heisenberg et al., *Nature* **405**, 76 (2000).
26. J. R. Jessen et al., *Nature Cell Biol.* **4**, 610 (2002).
27. E. S. Weinberg et al., *Development* **122**, 271 (1996).
28. Supported by grants from the March of Dimes Foundation (H.-y.W.), NIH (to C.C.M., to D.C.S.), the Ward Melville Walk-for-Beauty Foundation (H.-y.W.), and Howard Hughes Medical Institute (to R.T.M.); an Institutional National Research Service Award (T32-DK07521 to A.A.) and a Mentored Minority Award from NIH (A.A.); and a March of Dimes Foundation Basil O'Conner Research Scholar award (D.C.S.). We acknowledge T. Westfall (University of Iowa, Iowa City) for technical assistance and the guidance of M. Goligorsky (New York Medical College, Valhalla) in enabling the calcium measurements of F9 cells.

Supporting Online Material

www.sciencemag.org/cgi/content/full/298/5600/2006/DC1

Materials and Methods  
Figs. S1 to S5  
Tables S1 to S3

9 May 2002; accepted 7 October 2002

## Resetting the Circadian Clock by Social Experience in *Drosophila melanogaster*

Joel D. Levine,<sup>1</sup> Pablo Funes,<sup>1,2</sup> Harold B. Dowse,<sup>3</sup> Jeffrey C. Hall<sup>1\*</sup>

Circadian clocks are influenced by social interactions in a variety of species, but little is known about the sensory mechanisms underlying these effects. We investigated whether social cues could reset circadian rhythms in *Drosophila melanogaster* by addressing two questions: Is there a social influence on circadian timing? If so, then how is that influence communicated? The experiments show that in a social context *Drosophila* transmit and receive cues that influence circadian time and that these cues are likely olfactory.

Circadian clocks in animals regulate the timing of molecular, physiological, and behavioral rhythms. Environmental features such as photoperiod and temperature cycles reset these biological oscillators, enabling

anticipation of dawn, dusk, and season (1–6). Other kinds of cues (“nonphotic”) also influence clock time (7). For example, studies on humans (8), rodents (9), fish (10), and bees (11) have demonstrated social influences on rhythmicity, but underlying sensory mechanisms remain unexplained. It is nonetheless clear that multiple sensory pathways transmit ambient temporal information from the periphery to clock cells in the brain (7).

We investigated social influence on circadian timing in the fruit fly *Drosophila melano-*

*gaster*. We initially hypothesized that the circadian phases [marked by the peak of locomotor activity in DD (constant darkness)] would be more coherent for *Drosophila* living together (group-housed) than those of isolates, because groups of flies might agree about the time of day even without photic cues. Locomotor activity rhythms from group-housed wild-type individuals were compared to those of sibling isolates. After an initial 5 days in 12 hours of light and 12 hours of dark (LD 12:12), isolates and group-housed subjects were maintained for 2 weeks in DD. Isolates were then placed in activity monitors, whereas the group-housed flies were separated and monitored in DD to assess the effects on individual rhythmicity (12).

The effect of this treatment on phase coherence was analyzed with the use of circular statistics (Fig. 1A) (13, 14). The resulting vector angle indicates the mean peak time for each group, and its magnitude indicates phase coherence, with longer tails denoting a tighter distribution of phase estimates around the day (0, no correlation; 1, perfect correlation) (13, 14). The difference in phase coherence was significant ( $P = 0.02$ ), and there was no effect on phase angle (timing) ( $P = 0.64$ ), suggesting that the clocks of group-housed individuals in DD are more synchronized than those of isolates (12).

<sup>1</sup>Department of Biology, Brandeis University, Waltham, MA 02454, USA. <sup>2</sup>Icosystem Corporation, 10 Fawcett Street, Cambridge, MA, 02138, USA. <sup>3</sup>Department of Biological Sciences and Department of Mathematics and Statistics, University of Maine, Orono, ME 04469, USA.

\*To whom correspondence should be addressed. E-mail: hall@brandeis.edu